Suppression of Conducted Emission Noise in Electric Vehicle Charger with Passive EMI Filter

Widyaningrum Indrasari
Department of Physics, Faculty of Mathematics and Natural Sciences, Universitas Negeri Jakarta

Shallu Fidhah Ariyanti
Department of Physics, Faculty of Mathematics and Natural Sciences, Universitas Negeri Jakarta

Tyas Ari Wahyu Wijanarko
Research Center for Testing Technology and Standard, National Research and Innovation Agency

Yoppy Yoppy
Research Center for Testing Technology and Standard, National Research and Innovation Agency

他

https://doi.org/10.5109/7326994

出版情報：Evergreen. 11 (4), pp.3618-3625, 2024-12. Interdisciplinary Graduate School of Engineering Sciences, Kyushu University, Japan
バージョン：

Suppression of Conducted Emission Noise in Electric Vehicle Charger with Passive EMI Filter

Widyaningrum Indrasari[1,*], Shallu Fidhah Ariyanti[1], Tyas Ari Wahyu Wijanarko[2,3,*], Yoppy Yoppy[2], Hutomo Wahyu Nugroho[2], Elvina Trivida[2], Haryo Dwi Prananto[2], Aditia Nur Bakti[2], Denny Hamdani[3], Muhammad Imam Sudrajat[2,4], Mohamad Khoirul Anam[2], Dwi Mandaris[2,5,*]

[1]Department of Physics, Faculty of Mathematics and Natural Sciences, Universitas Negeri Jakarta, Indonesia

[2]Research Center for Testing Technology and Standard, National Research and Innovation Agency, Indonesia

[3]School of Electrical Engineering and Informatics, Bandung Institute of Technology, Bandung 40132, Indonesia

[4]University of Twente, the Netherlands

[5]Electrical Engineering Department, Mercu Buana University, Indonesia

*Author to whom correspondence should be addressed:
E-mail: widyaningrum-indrasari@unj.ac.id; tyas005@brin.go.id; dwim003@brin.go.id

(Received May 13, 2024; Revised November 28, 2024; Accepted December 17, 2024).

Abstract: The EV battery charger system has the potential to generate significant EMI noise due to the fast-switching process of the AC-DC converter. It may cause interferences to the operation of other electronic devices nearby. In this paper, a passive Pi-based filter was developed to mitigate EMI and to reduce conducted emission (CE) noise on an EV charger system. The filter design process was guided by a systematic approach where firstly the differential mode (DM) and common mode (CM) components of conducted emissions were separated and measured. After that, the required level of attenuation was calculated according to the standard's limits. Based on the needed attenuation level, the DM and CM filter component values were calculated and simulated. After obtaining the optimized component values, the filter was implemented. Measurement results showed that the proposed Pi filter effectively suppresses the EMI noise up to 43.40 dBµV/m resulting in the CE noise level met the EMC standard.

Keywords: Conducted Emission; Noise; EV Charger; passive filter; EMI

1. Introduction

The transition from combustion engines to electric vehicles (EV) has been developed massively to reduce dependence on fossil fuels and utilize more environmentally friendly transportation[1–3]. In EV applications, combustion engines, fuel tanks, and exhaust systems are replaced by EV components such as inverters, battery packs, controllers, motor drives, and electric motors.

The development of EV comes with several challenges, including the issue of electromagnetic interference (EMI)[4–6]. In EV, EMI is induced by the use of fast-switching *dV/dt* and *dI/dt* electrical components, e.g., motor drive, inverter, DC-DC converter, etc[7–9]. Moreover, non-linear components such as transistors, diodes, capacitors, and inductors have significant contributions to the characteristics of noise from EV. Specifically, the common EMI noise from EV is generated during the battery charging process[10–12]. Moreover, EMI noise during the charging process can propagate through conduction to the grids and affect the performance of other interconnected electrical equipment[13,14]. During the charging process, EV battery charger draws electric current with rapid changes and high voltage[4,15,16]. These rapid changes cause EMI noise that can be coupled and flow through conductors in the form of conducted emission[17,18].

Several techniques to identify and prevent conducted emission (CE) noise have been extensively investigated. A study in[19] presented a method to analyze the source of CE in common mode (CM) and differential mode (DM) noise by extracting the impedances of the power mains, LISN, EUT, and cable connection with an in-circuit measurement on two inductive coupling probes in Switched-Mode Power Supplies (SMPS) through simulation and experimentation. The results showed that the proposed method can effectively 99,7% investigate the causes of CE noise. Another study proved that the inverter in the PV off-grid system causes CE noise to the output voltage[20]. To reduce the unwanted CE noise, Mohammad et al presented a passive EMI Filter to attenuate CM from an adjustable-speed alternating current (AC) motor drive.

This method can effectively reduce the peak load noise[21]. In other studies, the various filter structures (L, T, or Pi; a single-stage or more) positioned at the power converter input or output showed that the optimized filter can reduce CM more effectively than the commercial filter. Besides that, the use of an inductor, choke, and Pi filter is also a promising method to reduce CM and DM noise of CE[22,23]. They have insertion loss of around 40 - 80 dBμV in the frequency range 300 kHz – 1.5 MHz[22,24]. However, the existing solutions and studies regarding the CE noise reduction by using filters have not been applied to the real EV charging systems.

In this paper, to reduce CE EMI from an EV battery charging system, the passive Pi filter with a single stage is developed using determination of CM and DM noise comparing to the EMI regulation method, CISPR 14-1. A discrimination network is needed to measure the DM and CM components separately, then the disturbances are monitored by spectrum analyzer. With this information, the required insertion loss can be calculate to choose the proper EMI filter circuit[25]. The value of each component in the Pi filter is selected based on the characteristic of CM and DM noise of the Device Under Test (DUT) before the filter is installed. This relatively simple filter has a good ability to suppress conducted EMI noise from EV chargers. Based on the CE measurement results, the spectrums of DUT with and without filter are compared to examine the filter effectiveness in suppressing EMI from the EV charger. Due to the EV charger being normally connected to the 220 V of house distribution, in this study, the applied test limit refers to CISPR 14-1, which the value is shown in Table 1[26].

Table 1. The Limit of CISPR 14-1 Standard.

Frequency (MHz)	**Quasi Peak Limit (dBμV)**
0.15-0.50	80-74
0.50-5.00	74
5.00-30.0	74

2. Method

CE measurement was performed using the AC-line impedance stabilization network (LISN), while a current probe was used to characterize CM and DM current noise. There are two main steps in this study. The first step is identifying the characteristics of CE noise of each operating mode and identifying the predominant noise source between the CM and DM. The second step is to design the CE filter based on the characteristics of the predominant noise. The third step is to examine the effectiveness of the CE filter. The AC-LISN has the aim to ensure that the measured noise on the spectrum analyzer unequivocally originates from the Device Under Test (DUT), as shown in Fig. 1. The CE laboratory test setup is shown in Fig. 2.

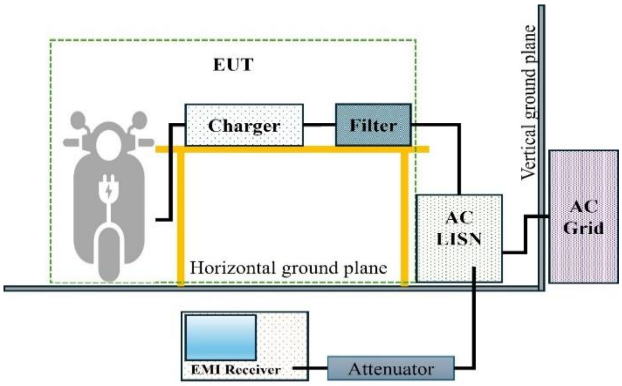

Fig. 1: Conducted Emission (CE) measurement.

In general, noise floor, ambient noise, cable type, cable length, EUT configuration, testing layout, LISN, and several other factors could affect CE spectrum[27]. However, this study is only focused on the variation of EV charger operations; thus, during the measurement, layout, cable type, and cable length are maintained in a fixed condition.

In the CE measurement, CE is categorized into two modes, L and N modes[19,28,29]. L mode is conducted on the phase line (L) of the AC system, where the line is carrying current from the power source. AC-LISN in L mode is connected with the phase path to measure the EMI generated by electronic devices on the phase path[30]. Meanwhile, the N mode is carried out on the neutral line (N). For this case, the EMI measurement on the neutral line is done by connecting the AC-LISN in N mode with the neutral line.

CM and DM measurements with the current probe Tekbox TBC P1 are carried out to investigate the current spectrum flowing in the cable. In CM measurement, the current probe is placed around both cables carrying the same current, where the current flows in the same direction in both conductors. Conversely, in DM measurement, the current probe is positioned around both cables with one cable wound around the current probe to obtain currents flowing in opposite directions.

In the charger testing, four configurations of CE measurement were performed, which are; the charger is connected to the battery offboard, the charger is connected to the whole EV system in the condition of not running (off), standby, and running (motor spinning). Therefore, the spectrum of CE, CM, and DM noise from the charger without a filter is obtained.

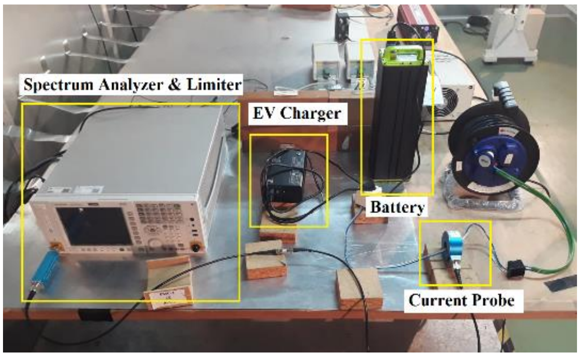

(a)

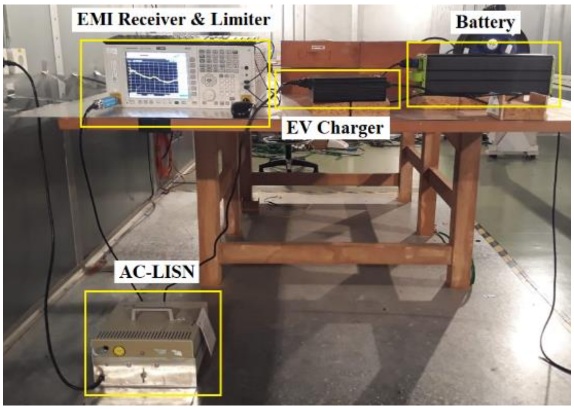

(b)

Fig. 2:(a) CM and DM measurement setup (b) CE Measurement setup.

The results obtained from this measurement are used to determine a proper filter design. In this study, a passive filter is employed to reduce CE noise in both CM and DM. The filter is developed based on Pi filter design due to its capability to handle high voltage and has a good ripple factor[31–33]. The proposed filter mainly consists of passive components such as inductors and capacitors to present impedance mismatch in the EMI current path as shown in Fig. 3[34]. Therefore, the filter characteristics depend upon the switching frequency and input/output impedance of the circuit. This filter operates by leveraging the reactive characteristics of the inductor and capacitor concerning frequency. At the desired frequency range, the inductor provides low impedance, while the capacitor provides high impedance, allowing signals at that frequency to pass through the circuit[34]. To achieve an effective filter, LTspice simulation is utilized to adjust the filter design to determine the cut-off frequency and calculate noise reduction at the range of 150 kHz to 30 MHz, as shown in Fig. 4. In this study, LTspice is preferred since it is free, relatively fast and has several tools to support comprehensive analysis.

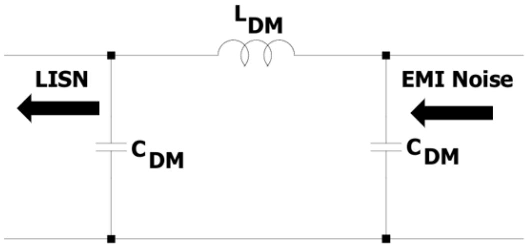

Fig. 3: Pi filter topology.

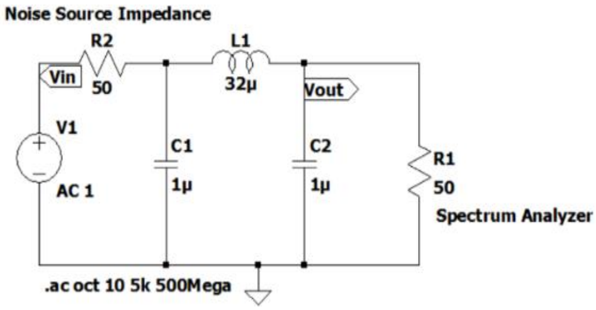

Fig. 4: LTspice Pi filter model.

In this study, the Pi filter is designed by specifying and calculating several key parameters to ensure it meets the desired performance criteria. The parameters considered in this study are desired attenuation (A_n) in dB, insertion loss (IL), cutoff frequency (f_c), capacitance value capacitor (C_1 and C_2), Inductance value of inductor (L), ripple voltage (V_{ripple}), and impedance matching. Eq. 1 is used to formulate the attenuation level. It is calculated based on the data samples with the highest noise and dB margin with the reference standards. The cutoff frequency is the frequency at which the filter starts to attenuate the signal. The relationship between f_c and the selection of the value of L and C is shown by Eq. 3. The value of L determines how effectively the filter can block high-frequency signals. A higher inductance value improves high-frequency attenuation. In the selection process of an inductor, it is essential to consider its maximum current rating (I_{rated}), saturation current, and DC resistance (DCR). Similarly, when selecting capacitors, it is essential to consider the voltage rating and the equivalent resistance series (ESR) of the capacitors. Capacitors with low ESR are preferred since they enhance the ability of the filter to attenuate the noise, reduce heat generation, and minimize power loss.

$$(V_{reg,DM})dB\mu V = (V_{DM})dB\mu V - (V_{limit})dB\mu V + (V_{margin})dB\mu V \quad (1)$$

$$f_c = f_{req} 10^{\left(\frac{-A_n}{20k}\right)} \quad (2)$$

$$f_c = 1/_{2\pi\sqrt{LC}} \quad (3)$$

Table 2. LTSpice simulation result: filter suppression level of various L and C configurations.

Config	Fixed Variable	Calculated	$R_2 = 50\ \Omega$	$R_2 = 1\ \Omega$
			Suppression (dB)	Suppression (dB)
1	$C_x = 0.56\ \mu F$	$L = 45.97\ \mu H$	54.96	27.89
2	$C_x = 0.68\ \mu F$	$L = 37.86\ \mu H$	56.65	28.29
3	$C_x = 1\ \mu F$	$L = 25.74\ \mu H$	59.99	29.49
4	$C_x = 3.3\ \mu F$	$L = 7.803\ \mu H$	70.37	36.85
5	$C_x = 6.8\ \mu F$	$L = 3.786\ \mu H$	76.64	42.78
6	$L = 32\ \mu H$	$C_x = 0.805\ \mu F$	58.12	28.75
7	$L = 43\ \mu H$	$C_x = 0.599\ \mu F$	55.56	28
8	$L = 58\ \mu H$	$C_x = 0.444\ \mu F$	52.97	27.56
9	$L = 68\ \mu H$	$C_x = 0.379\ \mu F$	51.61	27.4
10	$L = 30\ \mu H$	$C_x = 0.858\ \mu F$	58.67	28.94

where L is in Henry (H), C is in Farad (F) and k is 2 and 3 when calculating the CM and DM filter cut-off frequencies. If the value of C_1 and $C2$ are equal then the value of $C = C_1 = C_2$. If the value of $C_1 \neq C_2$, then the value of C is equivalent to $\sqrt{C_1 C_2}$. In this study, the value of the inductor and capacitor components is determined by simulation in LTspice to obtain the optimum attenuation of the selected frequency range. The $C_1 = C_2$ is preferred due to its symmetrical performance. An equal capacitor value ensures that the filtering action is balanced on both sides of the inductor. It also has better impedance matching because the impedance seen by the inductor is symmetrical.

3. Result and Discussions

Figsure 5(a) and (b) show the CM and DM noise spectrum of DUT under various charging conditions when no EMI filter is applied. The black line in Figs. 5(a) and (b) is the quasi-peak limit of CISPR 14-1 EMC standard, above which a CE measurement result is fail. Both DM and CM noise show high-level emissions, specifically, DM noise tends to have a high level at almost all frequencies due to the nature of EMI characteristic of the EV charging system. Also, the DM current path is basically independent of the system's dimensions as it always flows straight from the phase to the load and then returns to the neutral line. Meanwhile, CM noise shows a different pattern when the DUT operates under different conditions. CM emissions tend to be lower when the EV charger is only connected to the battery. This is because the battery is obviously much smaller in size compared to the complete EV, which means that the CM parasitic capacitance is also smaller compared to that of the complete EV. Furthermore, the highest CM emissions occur when the EV charging system is connected to the EV in the off condition. This high CM noise occurs because the charging system continues to work even though the EV is turned off. When charging, coupling noise occurs between the charging system and the components in the EV, both physical and parasitic components. This causes unwanted CM current looping.

Figure 6 and Fig. 7 showed the CE measurement results using an AC-LISN. Referring to Fig. 6(a) and 7(a), under all conditions, the CE measurement with AC-LISN indicates that the DUT generates noise that exceeds the limits in the frequency range of 150 kHz to 4 MHz. At a frequency higher than 4MHz, the noise gradually decreases to reach 42 dBµV.

From the CM and DM noise identification using the current probe at 150 kHz, the highest noise occurs at the differential mode, which is 104.78 dBµV during the charger connected to the battery. Therefore, the developed filter aimed to reduce DM noise. Compared to the standard limits at the required frequency of 150 kHz, an attenuation of 40.779 dBµV is needed. According to Eq. 1, the filter cut-off frequency is calculated to be 31.365 kHz. Then, the filter's inductor and capacitor values are determined using Eq. 3, in which one variable (either L or C) should be fixed and the other is calculated. Table 2 shows various combinations of inductors and capacitors where the column 'Fixed Variable' lists the available physical components. The actual value of noise source impedance R_2 is unknown. But most likely it is a low impedance because at the input of EV charger is a capacitor bank. For exploration purpose, the value of R_2 is chosen as 50 Ω and 1 Ω to reasonably represent the case of high and low impedance, respectively. Then, each calculated filter is simulated in LTSpice, and the suppresion levels at 150 kHz are listed in Table 2. Note that lower R_2 impedance results in less effective filter suppression.

Furthermore, to obtain the proper EMI filter, it is important to consider the voltage and current ratings of the EV charger. In this system, the charger has an input of 200-240 V_{AC} with the output voltage and current are 83 V_{DC} and 5 A, respectively. To determine the proper value of the Pi filter the magnitude of I_{rated} needs to be calculated. Then, an inductor is chosen with I_{rated} should be greater than 1.89 A to prevent component damage when it is exposed to the AC current flow. Also, leaded toroidal line choke inductors are chosen because the ferromagnetic materials of the inductor can increase the inductance and efficiency while reducing magnetic flux leakage. Furthermore, a film-type capacitor was chosen due to its good insulation properties, resistance to high temperatures, and stability in various environmental conditions.

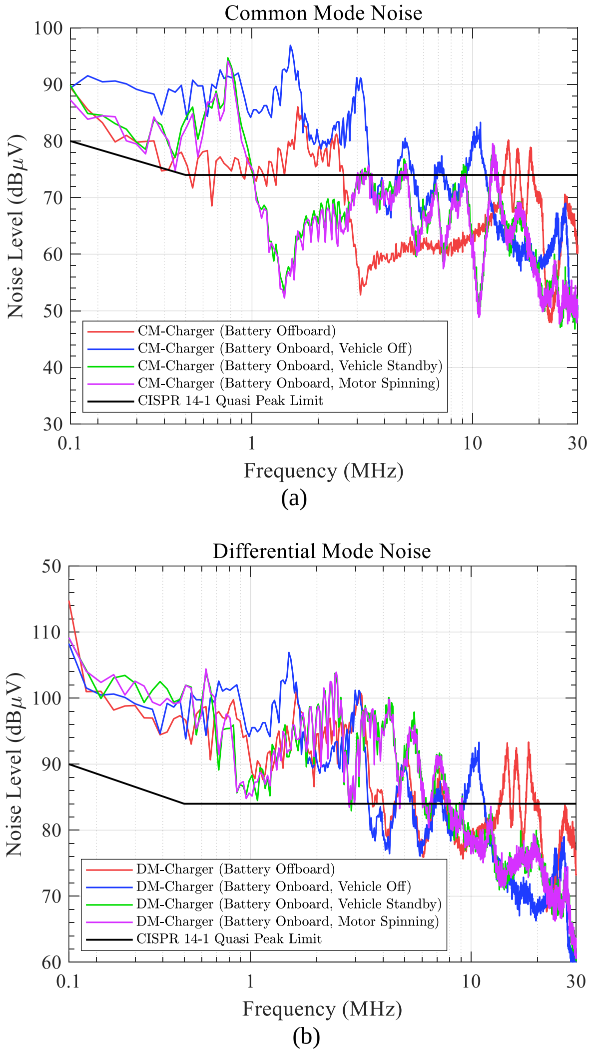

Fig. 5: CE spectrum EUT without filter (a) CM and (b) DM.

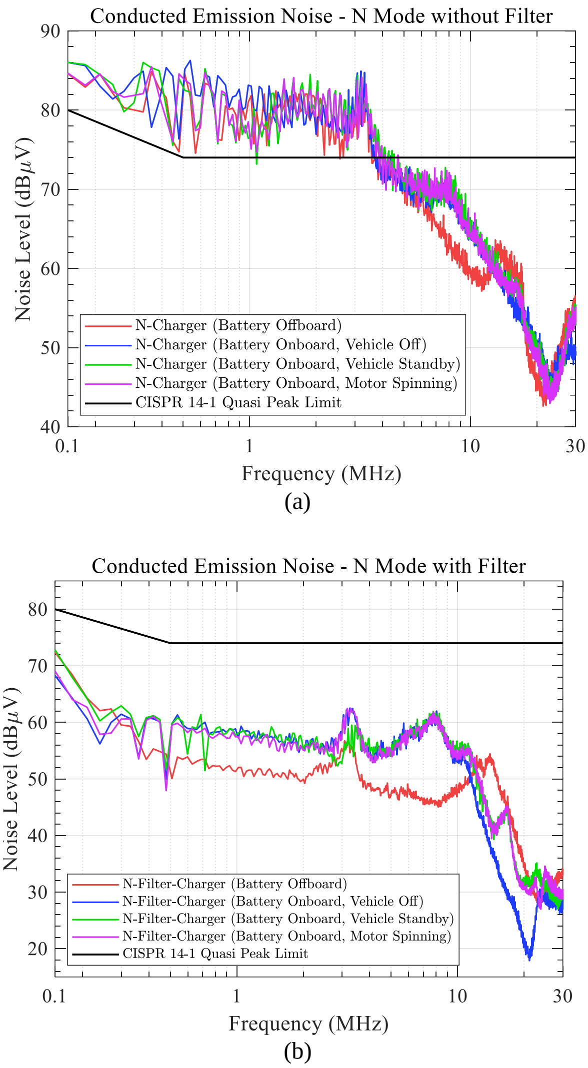

Fig. 6:(a) CE-N-mode without filter (b) CE-N mode with filter.

Configurations number 4 and 5 have the highest suppression levels, but they cannot be used because the inductor values are not available in the market. As an alternative, the filter with the largest damping results is configuration number 6 with L = 32 μH; C_x = 0.805 μF and configuration number 10 with L = 30 μH; C = 0.858 μF. Based on the datasheet, the 32 μH inductor has I_{rated} = 2.6 A and the 30 μH inductor has I_{rated} = 3.7 A. The larger I_{rated} comes with larger dimensions of the inductor. To avoid the use of components with unnecessary large dimensions, a value of L = 32 μH is used, and C = 1μF is used in place of 0.805 μF as in configuration number 6. Then, the filter is implemented and is placed at the AC input of EV charger to attenuate noise generated from both the charger and the complete EV.

The effectiveness of implemented filter is depicted in Figs. 6(b) and 7(b). It can be seen that the filter succeeded in reducing CE noise in both L and N mode types of measurements. At frequencies of 150 kHz to 5 MHz, the filter reduces noise significantly up to 43 dBμV. In particular, for the DM mode suppression level, the filter works very well and covers all frequency ranges. The frequency of the reduced CE emission is inline with the intended design of the filter, which is at the frequency response of 150 kHz to 30 MHz. However, the CE emission of the L and N at above 5 MHz is slightly no affected, this can be caused by the parasitic element of the inductor and capacitor in higher frequency used in the filter. Overall, the filter works so efficiently to reduce CE noise in the EV charger system that the CISPR 14-1 standard is met and compared to the other methods[23,31,33]), the results indicate that the method proposed in this research is more efficient and significant to suppress the conducted emission noise.

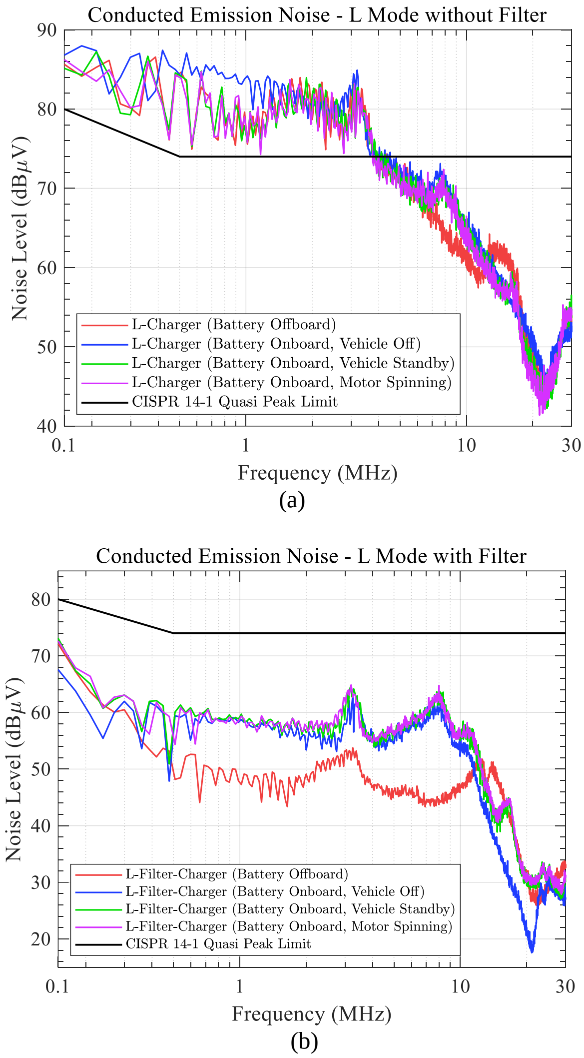

Fig. 7:(a) CE L-mode without filter (b) CE L-mode with filter.

4. Conclusions

The aim of this study was to design a filter to mitigate EMI on electric vehicle applications. The most important factor when analyzing EMI on EVs is the disparity in EMI level when EV is operated in various operating modes. In designing EMI filters effectively, engineers must observe this disparity and determine the highest EMI from various operating conditions. In this study, the filter has been developed based on a simple passive RLC Pi filter concept. This configuration is chosen due to the high level of DM noise, and also, the characteristic of the DM noise represents the nature of CE of the EV charging system. The measurement results indicate that the filter effectively suppresses CE EMI with a maximum attenuation of approximately 43.40 dBμV/m in the frequency range of 150 kHz to 30 MHz under battery load, ensuring compliance with the standard limit. Moreover, the addition of this filter can optimize charger performance in supplying electric power to the EV. In future research, the key area of focus is the optimization of the filter to get better attenuation on the frequency below 10 MHz. Future research will design the filter in the complete module, including prototyping PCB, selecting the precision component, and implementing it in the real mains supply for EV charging stations. Future research will also consider exploring the filter for different EV charger supply power rates.

Acknowledgements

The authors wish to gratefully acknowledge the encouragement and guidance of this research for the Department of Physics of Universitas Negeri Jakarta, and the Research Center for Testing Technology and Standard, National Research and Innovation Agency.

References

1) F. Hoeft, “Internal combustion engine to electric vehicle retrofitting: potential customer’s needs, public perception and business model implications,” *Transp. Res. Interdiscip. Perspect.*, **9** 100330 (2021). doi:10.1016/j.trip.2021.100330.
2) R.V. Petrescu, R. Aversa, A. Apicella, and F.I. Petrescu, “Friendly Environmental Transport,” *Am. J. Eng. Appl. Sci.*, **11** (*1*) 154–165 (2018). doi:10.3844/ajeassp.2018.154.165.
3) S.D. Musa, T. Zhonghua, A.O. Ibrahim, and M. Habib, “China’s energy status: A critical look at fossils and renewable options,” *Renew. Sustain. Energy Rev.*, **81** 2281–2290 (2018). doi:10.1016/j.rser.2017.06.036.
4) R. Kumar, C. Singh, V.R. Vakacharla, N. Tiwari, and T. Panwar, "Conductive and Inductive Charging for EVs Technologies, Standards: A Review" In: 2024 IEEE 3rd International Conference on Electrical Power and Energy Systems (ICEPES), 2024: pp. 1-6. doi:10.1109/ICEPES60647.2024.10653538.
5) Y.-M. Yang, H.-M. Peng, and Q.-D. Wang, “Common Model EMI Prediction in Motor Drive System for Electric Vehicle Application,” *J. Electr. Eng. Technol.*, **10** (*1*) 205–215 (2015). doi:10.5370/JEET.2015.10.1.205.
6) S. Jeschke, H. Hirsch, M. Trautmann, J. Bärenfänger, M. Maarleveld, M. Obholz, and J. Heyen, “EMI Measurement on Electric Vehicle Drive Inverters using A Passive Motor Impedance Network,” in: 2016 Asia-Pac. Int. Symp. Electromagn. Compat. APEMC, IEEE, 2016: pp. 292–294. https://ieeexplore.ieee.org/abstract/document/7523037/ (accessed May 7, 2024). doi:10.1109/APEMC.2016.7523037.
7) J. Hu, X. Xu, D. Cao, and G. Liu, “Analysis and Optimization of Electromagnetic Compatibility for Electric Vehicles,” *IEEE Electromagn. Compat. Mag.*, **8** (*4*) 50–55 (2019). doi:10.1109/MEMC.2019.8985599.
8) M. Al Sakka, J. Van Mierlo, H. Gualous, and U. Brussel, “DC/DC Converters for Electric Vehicles,” *Electr. Veh.-Model. Simul.*, **100** 466 (2011). doi: 10.5772/17048.
9) S. Wang, Y.Y. Maillet, F. Wang, D. Boroyevich, and

R. Burgos, “Investigation of Hybrid EMI Filters For Common-Mode EMI Suppression in A Motor Drive System,” *IEEE Trans. Power Electron.*, **25** (*4*) 1034–1045 (2009). doi:10.1109/TPEL.2009.2033601.

10) Y. Guo, L. Wang, and C. Liao, “Modeling and Analysis of Conducted Electromagnetic Interference in Electric Vehicle Power Supply System,” *Prog. Electromagn. Res.*, **139** 193–209 (2013). doi:10.2528/PIER13031101.
11) A.N. Bakti, Y. Yoppy, Y. Yudhistira, H.W. Nugroho, B. Utomo, D. Mandaris, D. Hamdani, T.D. Rachmilda, and F.A Nurman, "Electromagnetic Interference Measurement and Analysis of The Solar Charge Controller and Electric Motorcycle," In: 2022 IEEE International Conference in Power Engineering Application (ICPEA), 2022: pp. 1-5. doi:10.1109/ICPEA53519.2022.9744667.
12) Z. Wei, G. Dong, X. Zhang, J. Pou, Z. Quan, and H. He, “Noise-Immune Model Identification and State-of-Charge Estimation for Lithium-Ion Battery using Bilinear Parameterization,” *IEEE Trans. Ind. Electron.*, **68** (*1*) 312–323 (2020). doi: 10.1109/TIE.2019.2962429.
13) C. Jettanasen, “Influence of Power Shielded Cable and Ground on Distribution of Common Mode Currents Flowing in Variable-Speed AC Motor Drive Systems,” in: 2010 Asia-Pac. Int. Symp. Electromagn. Compat., IEEE, 2010: pp. 953–956. https://ieeexplore.ieee.org/abstract/document/5475550/ (accessed January 10, 2024). doi:10.1109/APEMC.2010.5475550.
14) G. Spadacini, F. Grassi, and S.A. Pignari, “Conducted Emissions in the Powertrain of Electric Vehicles,” in: 2017 IEEE Int. Symp. Electromagn. Compat. SignalPower Integr. EMCSI, IEEE, 2017: pp. 1–28. https://ieeexplore.ieee.org/abstract/document/8078064/ (accessed January 10, 2024). doi:10.1109/ISEMC.2017.8078064.
15) A. Kuperman, U. Levy, J. Goren, A. Zafransky, and A. Savernin, “Battery Charger for Electric Vehicle Traction Battery Switch Station,” *IEEE Trans. Ind. Electron.*, **60** (*12*) 5391–5399 (2012). doi:10.1109/TIE.2012.2233695.
16) Y.H. Lee, and A. Nasiri, “Analysis and Modeling of Conductive EMI Noise of Power Electronics Converters in Electric and Hybrid Electric Vehicles,” in: 2008 Twenty-Third Annu. IEEE Appl. Power Electron. Conf. Expo., IEEE, 2008: pp. 1952–1957. https://ieeexplore.ieee.org/abstract/document/4522995/ (accessed May 7, 2024). doi:10.1109/APEC.2008.4522995.
17) M. Pahlevaninezhad, D. Hamza, and P.K. Jain, “An Improved Layout Strategy for Common-Mode EMI Suppression Applicable to High-Frequency Planar Transformers in High-Power DC/DC Converters used for Electric Vehicles,” *IEEE Trans. Power Electron.*, **29** (*3*) 1211–1228 (2013). doi:10.1109/TPEL.2013.2260176.
18) H. Akagi, and T. Shimizu, “Attenuation of Conducted EMI Emissions from An Inverter-Driven Motor,” *IEEE Trans. Power Electron.*, **23** (*1*) 282–290 (2008). doi:10.1109/TPEL.2007.911878.
19) K.-R. Li, K.-Y. See, and R.M.S. Bandara, “Impact Analysis of Conducted Emission Measurement without LISN,” *IEEE Trans. Electromagn. Compat.*, **58** (*3*) 776–783 (2016). doi:10.1109/TEMC.2016.2533539.
20) D. Mandaris, H.W. Nugroho, P. Bakti, B. Utomo, T.A. Wahyu, S.W. Hidayat, F.A. Nurman, T.D. Rachmilda, and D. Hamdani, “Karakterisasi Conducted Emission Noise pada Inverter di Sistem Photovoltaic Off-Grid,” *J. Nas. Tek. Elektro Dan Teknol. Inf.*, **10** (*1*) 100–109 (2021). doi:10.22146/jnteti.v10i1.1066.
21) F. Mohammadi, G.-A. Nazri, and M. Saif, “A Bidirectional Power Charging Control Strategy for Plug-In Hybrid Electric Vehicles,” *Sustainability*, **11** (*16*) 4317 (2019). doi:10.3390/su11164317.
22) P.V.Y. Jayasree, J.C. Priya, G.R. Poojita, and G. Kameshwari, “EMI Filter Design for Reducing Common-Mode and Differential-Mode Noise in Conducted Interference,” *Int. J. Electron. Commun. Eng.*, **5** (*3*) 319–329 (2012).
23) H. Hizarci, U. Pekperlak, and U. Arifoglu, “Conducted Emission Suppression using An EMI Filter for Grid-Tied Three-Phase/Level T-Type Solar Inverter,” *IEEE Access*, **9** 67417–67431 (2021). doi:10.1109/ACCESS.2021.3077380.
24) G. Giglia, G. Ala, M.C. Di Piazza, G.C. Giaconia, M. Luna, G. Vitale, and P. Zanchetta, “Automatic EMI Filter Design for Power Electronic Converters Oriented to High Power Density,” *Electronics*, **7** (*1*) 9 (2018). doi:10.3390/electronics7010009.
25) V. Tarateeraseth, “EMI filter design: Part III: Selection of Filter Topology for Optimal Performance,” *IEEE Electromagn. Compat. Mag.*, **1** (*2*) 60–73 (2012). doi: 10.1109/MEMC.2012.6244975.
26) “CISPR 14 1 Electromagnetic Compatibility-Requirements for Household Appliances, Electric Tools and Similar Apparatus-Part 1: Emission,” (2020).
27) M.I. Sudrajat, M.A. Wibisono, N. Moonen, and F. Leferink, “Conducted Emission of a DC Motor Speed Drive: an Approach on Risk Assessment for Ship Application,” in: 2023 IEEE 7th Glob. Electromagn. Compat. Conf. GEMCCON, 2023: pp. 54–55. doi:10.1109/GEMCCON57842.2023.10078192.
28) K.L. Kaiser, “Electromagnetic Compatibility Handbook,” CRC press, 2004. https://books.google.com/books?hl=id&lr=&id=nZzOAsroBIEC&oi=fnd&pg=IA2&dq=handbook+electromagnetic+compatibility&ots=bD_GcySKZR&sig=cLM3AqcuvNuNMp1oGBKvMdyb3TU (accessed January 10, 2024).
29) S. Çakir, O. Sen, M. Çinar, and M. Çetintas, “Alternative Conducted Emission Measurements for Industry,” in: 2014 Int. Symp. Electromagn. Compat., IEEE, 2014: pp. 1037–1042. https://ieeexplore.ieee.org/abstract/document/6931055/ (accessed May 7, 2024). doi:10.1109/EMCEurope.2014.6931055.

30) S. Nitta, “Roles and Problems of LISN in Noise Measurement,” *IEICE Trans. Commun.*, **78** (*2*) 109–119 (1995).
31) V.S.C. Pathala, and V.Y. Pappu, “Elimination of CM Noise from SMPS Circuit using EMI Filter,” *Int. J. Electr. Comput. Eng. Syst.*, **14** (*4*) 465–471 (2023). doi:10.32985/ijeces.14.4.10.
32) J. Ji, W. Chen, X. Yang, X. Zhang, and N. Zhi, “A Layout Method of Passive EMI Filter,” in: 2017 IEEE Energy Convers. Congr. Expo. ECCE, IEEE, 2017: pp. 2346–2349. https://ieeexplore.ieee.org/abstract/document/8096455/ (accessed January 10, 2024). doi:10.1109/ECCE.2017.8096455.
33) E. Şehirli, “Examining the Design of Different Types of DM EMI Filters and Their Effect on EMI Noise and Control Characteristics for Cuk DC-DC Converter,” *Int. Trans. Electr. Energy Syst.*, **2023** (2023). https://www.hindawi.com/journals/itees/2023/7101065/ (accessed January 10, 2024). doi:10.1155/2023/7101065.
34) K.H. Ahmed, S.J. Finney, and B.W. Williams, “Passive Filter Design for Three-Phase Inverter Interfacing in Distributed Generation,” in: 2007 Compat. Power Electron., 2007: pp. 1–9. doi:10.1109/CPE.2007.4296511.